Supporting Information

Toward Design of Synergistically Active Carbon-Based Catalysts for Electrocatalytic Hydrogen Evolution

Yao Zheng[1,2,†], Yan Jiao[1, †], Lu Hua Li[3], Tan Xing[3], Ying Chen[3], Mietek Jaroniec[4], Shi Zhang Qiao[1*]

1 School of Chemical Engineering, University of Adelaide, Adelaide, SA5005, Australia.

2 Australian Institute for Bioengineering and Nanotechnology, University of Queensland, Brisbane, QLD 4072, Australia.

3 Institute for Frontier Materials, Deakin University, Waurn Ponds, VIC 3216, Australia.

4 Department of Chemistry and Biochemistry, Kent State University, Kent, Ohio 44242, USA.

Emial: s.qiao@adelaide.edu.au

[†]These authors contributed equally.

Part I Computational Section

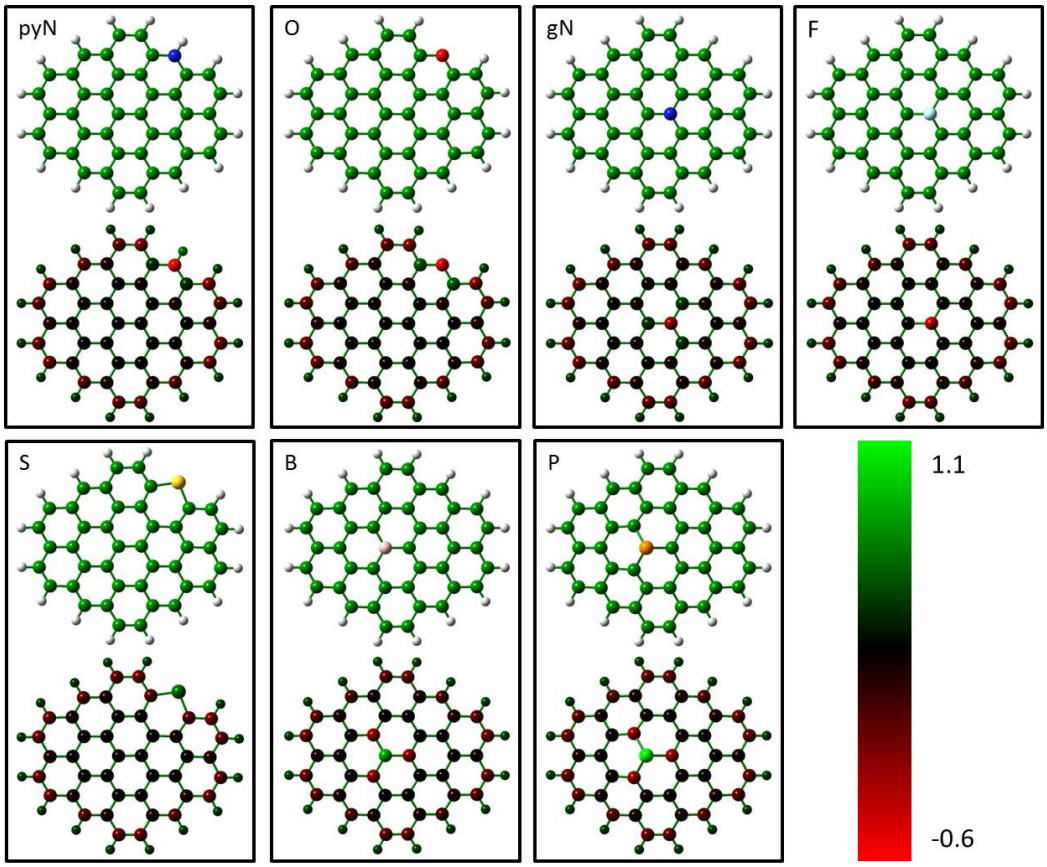

Figure S1. Molecular structures (top) and the corresponding NBO charge density distributions (bottom) of different heteroatoms single-doped graphenes.

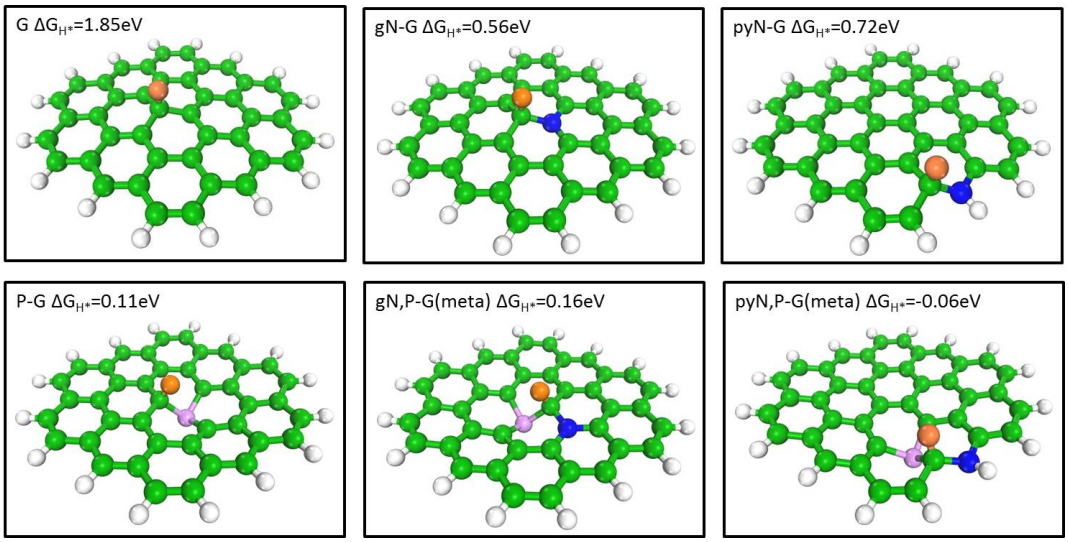

Figure S2. Hydrogen adsorption sites and configurations on different N (blue color) and/or P (pink color) doped graphenes, corresponding to Figure 1b.

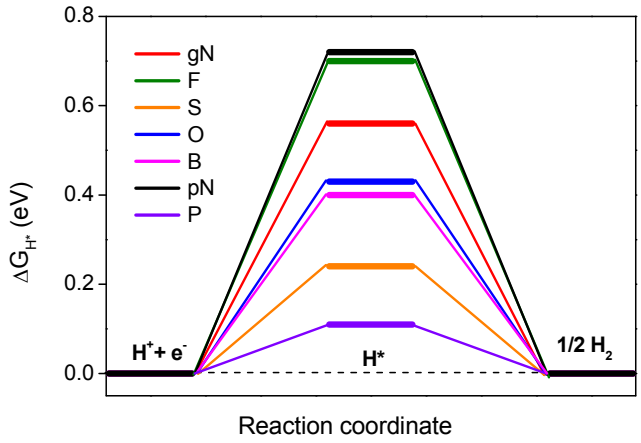

Figure S3. The calculated free-energy (ΔG_{H^*}) diagram of HER at the equilibrium potential (U_{RHE}=0 V) for various single-doped graphene models. The molecular configurations are shown in Figure S1.

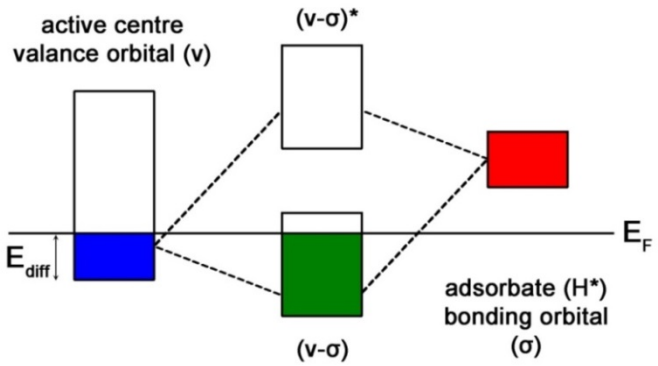

Scheme S1. The scheme of orbital hybridization of valance band for HER active sites (carbon atoms) and H* bonding orbital. E_F represents the Fermi energy level in the form of Natural Atomic Orbitals.

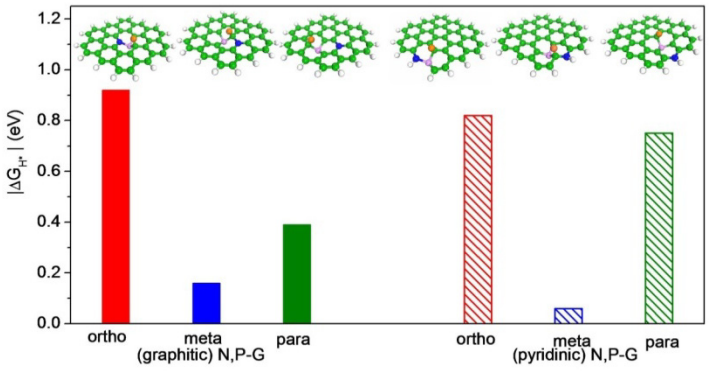

Figure S4. Hydrogen adsorption free energies and active sites (inset) on different N,P co-doped graphene configurations with pyridinic or graphitic N groups. Ortho, Meta, Para indicates the relative positions of N (blue color) and P (pink color) heteroatoms in one benzene heteroring.

Part II: Experimental Section

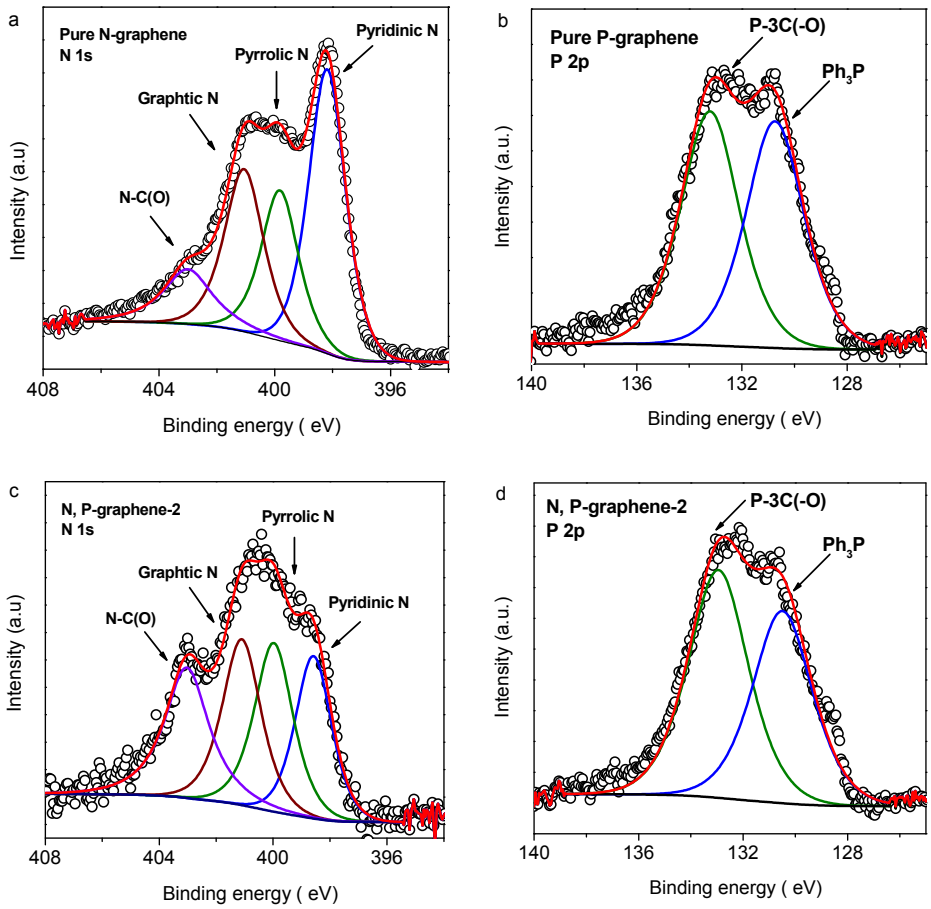

Figure S5. High-resolution XPS of (a) pure N-graphene (N1s), (b) pure P-graphene (P2p), (c, d) two-step synthesized N,P-graphene-2 (first incorporating P then N) in which there was a large amount O-containing groups in both N and P species. Note that if N is incorporated first, P could not form the N,P co-doped graphene but only N-graphene (see the aforementioned material synthesis procedure; the XPS spectra were very similar to those of N-graphene and therefore not shown here).

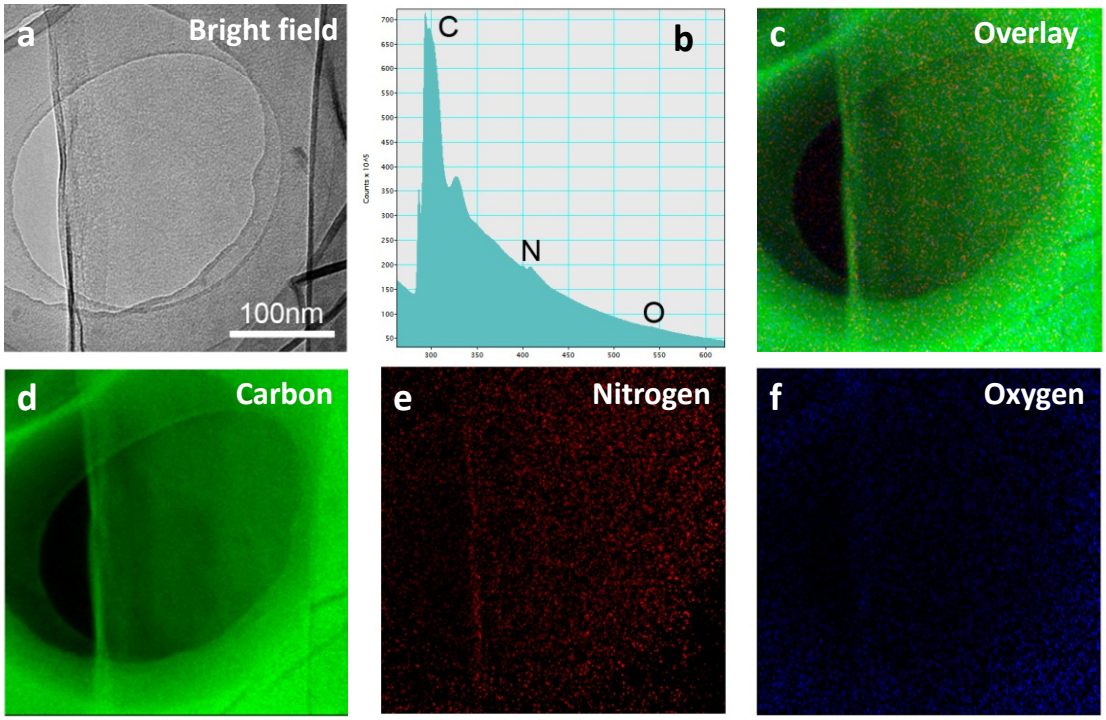

Figure S6. EELS mapping of a N,P-graphene-1 nanosheet. (a) Bright image and (b-f) EELS spectrum and elemental maps of C, N, O. P's L-edge signal is too weak to be detected due to its low doping concentration (~1.6 %)

Table S1 Electrochemical analysis of different catalysts based on polarization curves and Tafel plot

0.5 M H_2SO_4	**On-site potential[a] (V, *vs.* RHE)**	**η @10 mA/cm^2 (V, *vs.* RHE)**	**Tafel slope (mV/dec)**	**i_0 (A/cm^2)**
N-graphene	0.331	0.490	116	$7.04*10^{-8}$
p-graphene	0.374	0.553	133	$8.97*10^{-9}$
N,P-graphene-1	0.289	0.422	91	$2.44*10^{-7}$
0.1 M KOH	**On-site potential (V, *vs.* RHE)**	**η @5 mA/cm^2 (V, *vs.* RHE)**	**Tafel slope (mV/dec)**	**i_0 (A/cm^2)**
N-graphene	0.396	0.633	143	$1.17*10^{-10}$
P-graphene	0.454	0.683	159	$1.64*10^{-11}$
N,P-graphene-1	0.389	0.585	145	$3.96*10^{-10}$

[a] The potential at which the hydrogen evolution occurrs, defined in this study as the overpotential at which reduction current density is 0.5 mA/cm^2 in acid solution and 0.25 mA/cm^2 in base solution.

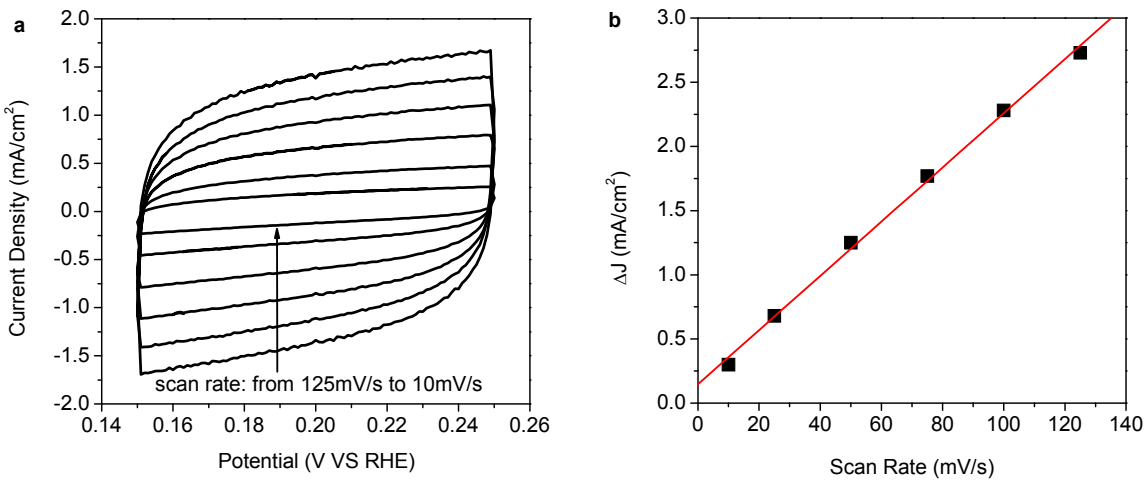

Figure S7 (a) CV curves and (b) corresponding differences in the current density at 0.2 V plotted against scan rate.

To perform the activity normalization, first we calculated the electrochemical active surface areas for the synthesized catalysts by measuring their electrochemical double layer capacitances (C_{dl}) using a simple CV method. A potential range of 0.15-0.25 V vs RHE was selected for the capacitance measurements because no obvious electrochemical features corresponding to Faradic current were observed in this region for each catalyst (Figure S7a). Then, the capacitive currents, i.e. $\Delta J_{|Ja-Jc|}$ @0.2 V were plotted as a function of CV scan rate, as shown in Figure S7; linear relationships were observed with the slope twice larger than the C_{dl} Value. This method gives the C_{dl} values for N,P-G-1 equal to 10.6 mF/cm^2 (Table S2).

Table S2 Summary of the normalized exchange current densities in relation to the catalyst loading and/or electrochemical active surface area on various nanostructured catalysts.

Catalysts	catalyst loading (μg/cm^2)	C_{dl} (mF/cm^2)	I_0 (A/cm^2)	C_{dl} normalized by mass	I_0 (A/cm^2) normalized by mass and area	Ref
MoS_2 Nanosheet	285	33.7	12.6×10^{-6}	2.2	5.6×10^{-6}	1
MoS_2/graphene	210	10.4	3×10^{-6}	0.93	3.2×10^{-6}	2
Amorphous MoS_3	~31	2.3	8.9×10^{-7}	1.4	0.63×10^{-6}	3
MoO_3-MoS_2 nanowire	60	2.2	0.82×10^{-7}	0.69	0.11×10^{-6}	4
Nanostructured MoS_2	60	4.8	6.9×10^{-7}	1.5	0.45×10^{-6}	5
Nanostructured MoS_2	60	1.1	1.3×10^{-7}	0.35	0.37×10^{-6}	5
Nanostructured MoS_2	60	2.7	2.6×10^{-7}	0.85	0.30×10^{-6}	5
N,P-G-1	200	10.6	2.4×10^{-7}	1	0.24×10^{-6}	This work

Assuming the value (catalyst loading or surface area) of N,P-G-1 as a reference, the relative i_0 of other metallic electrocatalysts are shown in Table S2. By considering the influence of the catalyst loading on the electrochemical active surface area for one catalyst, it is more reasonable to normalize i_0 to both mass and surface area as shown in the last column of Table S2, where one can see that the activity of N,P-G-1 is "comparable" to those of the well-developed nanostructured MoS_2-based metallic catalysts (with in an order of magnitude).

References

1. Xie, J.; Zhang, J.; Li, S.; Grote, F.; Zhang, X.; Zhang, H.; Wang, R.; Lei, Y.; Pan, B.; Xie, Y. Controllable Disorder Engineering in Oxygen-Incorporated MoS_2 Ultrathin Nanosheets for Efficient Hydrogen Evolution. *J. Am. Chem. Soc.* **2013**, 135, 17881.
2. Liao, L.; Zhu, J.; Bian, X.; Zhu, L.; Scanlon, M.; Girault, H.; Liu, B. MoS_2 Formed on Mesoporous Graphene As a Highly Active Catalyst for Hydrogen Evolution. *Adv. Funct. Mater.* **2013**, *23*, 5326.
3. Merki, D.; Vrubel, H.; Rovelli, L.; Fierro, S.; Hu, X. Fe, Co, and Ni Ions Promote the Catalytic Activity of Amorphous Molybdenum Sulfide Films for Hydrogen Evolution. *Chem. Sci.* **2012**, *3*, 2515.
4. Chen, Z.; Cummina, D.; Reinecke, B.; Clark, E.; Sunkara, M.; Jaramillo, T. Core-Shell MoO_3-MoS_2 Nanowires for Hydrogen Evolution: A Functional Design for Electrocatalytic Materials. *Nano Lett.* **2011**, *11*, 4168.
5. Kibsgaard, J.; Chen, Z.; Reinecke, B. N.; Jaramillo, T. F. Engineering the Surface Structure of MoS_2 to Preferentially Expose Active Edge Sites for Electrocatalysis. *Nat. Mater.* **2012**, *11*, 963.